Int. J. Solids Structures, 1977, Vol. 13, pp. 981–993. Pergamon Press. Printed in Great Britain

APPLICATION OF BOUNDS FOR CREEPING STRUCTURES SUBJECTED TO LOAD VARIATIONS ABOVE THE SHAKEDOWN LIMIT

R. A. AINSWORTH

Central Electricity Generating Board, Berkeley Nuclear Laboratories, Berkeley, Gloucestershire, England

(*Received* 15 *November* 1976; *revised* 5 *April* 1977)

Abstract—Previous work established upper bounds on work and displacement for creeping structures subjected to load variations above the shakedown limit. The present paper applies these bounds to three structures subjected to constant mechanical loading and to variable imposed strains. The results are in good agreement with those of more detailed calculations.

NOTATION

α	coefficient of thermal expansion
β	non-dimensional strain $\{\beta = E\epsilon/\sigma_y\}$
γ	non-dimensional curvature $\{\gamma = E\kappa h/2\sigma_y\}$
ϵ, ϵ_{ij}	strain
ζ	non-dimensional distance $\{\zeta = z/h\}$
θ	temperature
κ	curvature
$\dot{\Lambda}$	plastic multiplier
λ	constant describing loading cycle
μ	load factor
ν	Poisson's ratio
Σ	non-dimensional stress $\{\Sigma = \sigma/\sigma_y\}$
$\sigma, \sigma_y, \sigma_0, \sigma_r, \sigma_p$	stress, yield stress and constant stresses, respectively
τ	cycle time
ϕ	stress function
A	area of bar
b	breadth of beam
$\dot{D}$	creep energy dissipation rate
E, E_1	elastic modulus and tangent modulus, respectively
e, e_{ij}	elastic strain
F	constant describing temperature effect
$f(\sigma_{ij})$	yield function
$g(\theta)$	positive function of temperature
h	depth of beam, thickness of tube
k	constant
l	length of bar
m	constant
n	creep index
P, P_i	applied loads
p, p_{ij}	plasitic strain
R	additional load, radius of tube
S	surface
S_{ij}	stress deviator tensor
T	temperature
T_{ij}	tensor $\{T_{ij} = S_{ij} - mp_{ij}\}$
t	time
t_1	non-dimensional time $\{t_1 = E\dot{V}_0 t/\sigma_y\}$
u, U	displacement
V	volume
$\dot{V}_{ij}, \dot{V}_0$	creep strain rate and constant strain rate, respectively
z	distance from centre-line of beam or tube

Subscripts

x, θ	axial and hoop components, respectively, for the tube.

1. INTRODUCTION

A problem of importance in the design of fast-reactor nuclear power plant is the behaviour of structures operating at high temperature which must withstand repeated changes of mechanical load and temperature. Some situations produce severe thermal gradients which violate shakedown conditions and it is necessary to carry out an inelastic analysis which allows both creep

and repeated plasticity. Although a full inelastic analysis could be carried out by computer methods, such an analysis is extremely expensive in computing time and is not suitable for normal design purposes.

In recent years, considerable attention has been paid to the development of approximate methods which obviate the need for a full inelastic analysis. The development of approximate methods and bounding techniques has been reviewed by Odqvist[1] for steady loading and by Leckie[2] for variable loading below the shakedown limit. The extension of the bounding technique of Ponter[3] (see also [2]) for load and temperature variations above the shakedown limit has recently been given by Ainsworth[4]. The bounding method relies on separating the elastic-plastic behaviour from the creep behaviour; the response within a cycle of loading is governed by elastic-plastic behaviour leading to a cycle of stress and the overall deformation due to creep is calculated from the creep strains due to this cycle of stress. It should be noted that the bounds are only strictly valid for simple non-interactive creep and plasticity laws in which effects such as creep recovery and cyclic hardening or softening are neglected. In the present paper, the use of these bounding methods is demonstrated by application to some simple structures and the results are compared with those of more detailed analysis.

2. MATERIAL BEHAVIOUR AND THEORETICAL RESULTS

The total strain rate $\dot{\epsilon}_{ij}$ is considered as the sum of four parts

$$\dot{\epsilon}_{ij} = \dot{e}_{ij} + \dot{V}_{ij} + \dot{p}_{ij} + \dot{\theta}_{ij} \tag{1}$$

where $\dot{e}_{ij}$, $\dot{V}_{ij}$, $\dot{p}_{ij}$, $\dot{\theta}_{ij}$ are elastic, creep, plastic and imposed (or thermal) strain rates respectively. Elastic strains are given by Hooke's law and creep strains are given in terms of a stress function ϕ by,

$$\dot{V}_{ij}/\dot{V}_0 = \phi^n\{\partial\phi/\partial(\sigma_{ij}/\sigma_0)\}g(\theta), \tag{2}$$

where n, σ_0, $\dot{V}_0$ are constants and $g(\theta)$ is a positive function of the temperature θ. Two types of plastic behaviour are considered. The first is one of perfect plasticity with yield criterion $f(\sigma_{ij}) \leq 0$ and the associated flow rule,

$$\dot{p}_{ij} = \dot{\Lambda}\,\partial f/\partial\sigma_{ij}, \tag{3}$$

where

$$\dot{\Lambda} = 0 \text{ if } f < 0 \text{ or if } f = 0 \text{ and } \{\partial f/\partial\sigma_{ij}\}\dot{\sigma}_{ij} < 0$$

$$\dot{\Lambda} \geq 0 \text{ if } f = 0 \text{ and } \{\partial f/\partial\sigma_{ij}\}\dot{\sigma}_{ij} = 0.$$

The second type of plastic behaviour considered is one of linear kinematic strain hardening with yield criterion,

$$T_{ij}T_{ij} - k^2 \leq 0 \text{ where } T_{ij} = S_{ij} - mp_{ij}, \tag{4}$$

where m and k are constants. The associated flow rule is,

$$\dot{p}_{ij} = \dot{\Lambda}T_{ij}, \tag{5}$$

where

$$\dot{\Lambda} = 0 \text{ if } T_{ij}T_{ij} < k^2 \text{ or if } T_{ij}T_{ij} = k^2 \text{ and } T_{ij}\dot{S}_{ij} < 0$$

$$\dot{\Lambda} = T_{ij}\dot{S}_{ij}/mk^2 \text{ if } T_{ij}T_{ij} = k^2 \text{ and } T_{ij}\dot{S}_{ij} \geq 0.$$

Consider a body of volume, V, surface, S, with negligible body forces and composed of material having the behaviour outlined above. The body is subjected to given imposed strains

$\theta_{ij}(t)$, to given mechanical loading $P_i(t)$ over part S_P of S, and to zero surface velocities over the remainder S_u of S. The imposed strains and mechanical loads both have period τ so that $\theta_{ij}(t+\tau) = \theta_{ij}(t)$ and $P_i(t+\tau) = P_i(t)$. It has been shown in [4] that the displacements $\dot{u}_i$ of such a structure can be bounded by cyclic plasticity solutions for a structure that does not creep. Denote by $\sigma_{ij}^{\dagger}$ a cyclic plasticity solution for a structure having imposed strains $\theta_{ij}(t)$ and applied loads $P_i(t) + R_i(t)$ where $R_i(t)$ are additional loads of period τ. If the additional loads R_i are taken as a constant point load $R(R > 0)$ the displacement U_R in the line of R is bounded by, [4],

$$U_R(\tau) - U_R(0) \leq U_R^{\dagger}(\tau) - U_R^{\dagger}(0) + \frac{1}{nR}\left(\frac{n}{n+1}\right)^{n+1} \int_0^{\tau}\int_V \dot{D}(\sigma_{ij}^{\dagger}/\sigma_0)\,\mathrm{d}V\,\mathrm{d}t, \tag{6}$$

where $\dot{D}(\sigma_{ij}/\sigma_0)$ is the creep energy dissipation rate $\sigma_{ij}\dot{V}_{ij}$ and where $U_R^{\dagger}$ is the displacement in the line of R associated with the cyclic plasticity solution. Setting the additional loads proportional to the applied loads as $R_i = (\mu - 1)P_i$ where μ is a constant ($\mu > 1$) gives a work bound, [4],

$$\int_0^{\tau}\int_s P_i\dot{u}_i\,\mathrm{d}S\,\mathrm{d}t \leq \int_0^{\tau}\int_s P_i\dot{u}_i^{\dagger}\,\mathrm{d}S\,\mathrm{d}t + \frac{1}{(\mu-1)n}\left(\frac{n}{n+1}\right)^{n+1}\int_0^{\tau}\int_V \dot{D}(\sigma_{ij}^{\dagger}/\sigma_0)\,\mathrm{d}V\,\mathrm{d}t, \tag{7}$$

where $\dot{u}_i^{\dagger}$ are the displacement rates associated with the cyclic plasticity solution.

The bounds (6, 7) can be optimised by choice of additional loads (R or μ) and by choice of the stress distribution $\sigma_{ij}^{\dagger}$. In the application to simple structures, optimum bounds are used and these are bounds for which the cyclic plasticity solution has an associated strain cycle,

$$\int_0^{\tau} [\dot{V}_0\phi^n\{\partial\phi/\partial(\sigma_{ij}^{\dagger}/\sigma_0)\}g(\theta) + \dot{\Lambda}\,\partial f/\partial\sigma_{ij}^{\dagger}]\,\mathrm{d}t \tag{8}$$

which is kinematically admissible. Here $\dot{\Lambda}$ are plastic multipliers, required only for perfectly-plastic materials, which satisfy $\dot{\Lambda} \geq 0$, $\dot{\Lambda} f(\sigma_{ij}^{*}) = 0$.

3. APPLICATION TO SIMPLE STRUCTURES

Three simple structures, a beam, a tube and a two-bar mechanism are considered. For all structures, the mechanical loads are held constant and there are periodic variations of imposed or thermal strains. These are the conditions most likely to violate shakedown for practical structures.

The uniaxial form of the elastic-plastic behaviour is shown in Fig. 1. The constants m, k of eqn (4) are related to the virgin yield stress σ_y and the slope E_1 by $k^2 = 2\sigma_y^2/3$ and $m = 2EE_1/3(E - E_1) \simeq 2E_1/3$.

Results are presented in non-dimensional form using a non-dimensional stress $\Sigma = \sigma/\sigma_y$, a non-dimensional strain $\beta = E\epsilon/\sigma_y$ and a non-dimensional time $t_1 = E\dot{V}_0 t/\sigma_y$. The arbitrary normalising stress σ_0 of eqn (2) is taken as the yield stress σ_y.

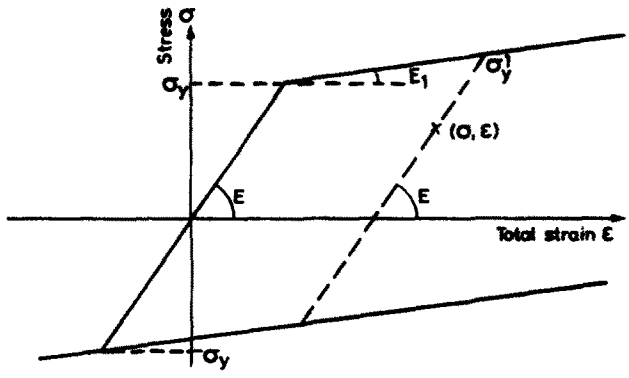

Fig. 1. Stress-strain curve.

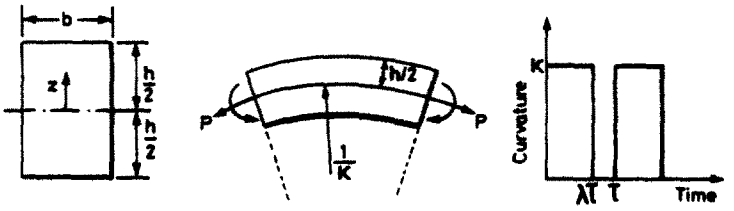

Fig. 2. Geometry and loading of beam.

3.1 *Rectangular section beam*

Consider the rectangular section beam shown in Fig. 2, subjected to a constant axial load P and a periodic curvature κ. The temperature is uniform throughout the beam and the temperature effect of eqn (2) is taken as $g(\theta) = 1$.

Exact solution–hardening material. During periods of creep at constant curvature, the total strain rate $\dot{\epsilon}$ is given from eqns (1) and (2) as

$$\dot{\epsilon} = \dot{\sigma}/E + \dot{V}_0(\sigma/\sigma_y)^n$$

where it is assumed that no further plastic strains occur during these parts of the cycle. (As expected, the peak stress relaxed and this assumption was found to be valid for the loading conditions considered.) Since the curvature and axial load are constant, the strain rate is uniform through the thickness and the mean stress rate is zero. Hence

$$\mathrm{d}\beta/\mathrm{d}t_1 = \int_{-1/2}^{1/2} \Sigma^n \,\mathrm{d}\zeta; \quad \partial\Sigma/\partial t_1 = \int_{-1/2}^{1/2} \Sigma^n \,\mathrm{d}\zeta - \Sigma^n \tag{9}$$

where the non-dimensional variables Σ, β, t_1 and $\zeta = z/h$ have been introduced. Representing the stress distribution by values at a number of points through the beam, eqn (9) has been solved using the method of time-steps (see for example, Penny and Marriott[5]). For a given time-step Δt_1 the new stress distribution Σ_{r+1}, say, at time $t_1 + \Delta t_1$ was found from the distribution Σ_r at time t_1 using a fourth-order Runge-Kutta method. Denoting the second of eqns (9) as $\partial\Sigma/\partial t_1 = f(\Sigma)$, then

$$\Sigma_{r+1} = \Sigma_r + (k_0 + 2k_1 + 2k_2 + k_3)/6 \tag{10}$$

where

$$k_0 = \Delta t_1 f(\Sigma_r), \quad k_1 = \Delta t f(\Sigma_r + \tfrac{1}{2}k_0), \quad k_2 = \Delta t_1 f(\Sigma_r + \tfrac{1}{2}k_1), \quad k_3 = \Delta t_1 f(\Sigma_r + k_2)$$

The method (10) was found to be more economical in computing time than the simple time-step method $\Sigma_{r+1} = \Sigma_r + \Delta t_1 f(\Sigma_r)$ which required a smaller value of allowable time-step to obtain consistent results.

The above elastic-creep analysis must be interrupted at times of curvature change by an elastic-plastic analysis. Denoting a change in curvature by $\Delta\kappa$, the total strain change is $\Delta\epsilon = \Delta\epsilon_0 + z\Delta\kappa$ where $\Delta\epsilon_0$ is the change in mean strain which must be found. Referring to Fig. 1, if the stress σ and the effective yield stress σ_y^1 are known, the stress and strain increments $\Delta\sigma, \Delta\epsilon$ are related by:

$$\text{if } \sigma = \sigma_y^1 \text{ and } \Delta\epsilon \geq 0, \ \Delta\sigma = E_1\Delta\epsilon \text{ and } \Delta\sigma_y^1 = E_1\Delta\epsilon$$

$$\text{if } \sigma_y^1 - 2\sigma_y \leq \sigma < \sigma_y^1 \text{ and } \Delta\epsilon > 0, \ \Delta\sigma = E\Delta\epsilon \text{ and } \Delta\sigma_y^1 = 0$$

$$\text{unless } \sigma + \Delta\sigma > \sigma_y^1 \quad \text{when } \Delta\sigma = \sigma_y^1 - \sigma + E_1[\Delta\epsilon - (\sigma_y^1 - \sigma)/E]$$

$$\text{and} \quad \Delta\sigma_y^1 = E_1[\Delta\epsilon - (\sigma_y^1 - \sigma)/E]$$

Similar conditions are applicable for $\Delta\epsilon < 0$. An estimate of $\Delta\epsilon_0$ was used to evaluate the

changes $\Delta\sigma$ and an iterative method was used to find that value of $\Delta\epsilon_0$ for which the mean stress change was zero (to within acceptable limits).

For perfectly-plastic and isotropic strain-hardening materials, the exact solution to the elastic-plastic problem has been obtained by Bree [6] and the results may be simply modified for kinematic hardening materials allowing for yielding in both tension and compression. Details of this are omitted for brevity but the results indicate that, even after a large number of curvature changes, no significant error is introduced by the numerical elastic-plastic analysis outlined above.

Combination of the above elastic-creep and elastic plastic analyses enables the cyclic stationary state to be obtained by convergence from any initial stress distribution. A typical solution is shown in Fig. 3 where the stress distribution is shown at various times (t_1) during the cycle. The mean strain rate occurring in the cyclic stationary state is shown for a range of non-dimensional cycle time τ and cycle parameter λ (see Fig. 2) in Fig. 4.

Upper displacement bound. In order to determine the upper bound (6), a cyclic plasticity solution must be evaluated. Introducing the non-dimensional curvature $\gamma = E\kappa h/2\sigma_y$ it can be seen that the elastic stress range is greater than $2\sigma_y$ for $|\zeta| > 1/\gamma$. Denoting the non-dimensional stress distribution for the cyclic plasticity solution as $\Sigma_1(\zeta)$ for $0 < t_1 < \lambda\tau$ and as $\Sigma_2(\zeta)$ for $\lambda\tau < t_1 < \tau$, then

$$\begin{aligned}
\Sigma_2(\zeta) &= \Sigma_1(\zeta) + 2 - 2E_1(\gamma\zeta + 1)/E, \quad -1/2 \le \zeta \le -1/\gamma \\
\Sigma_2(\zeta) &= \Sigma_1(\zeta) - 2\gamma\zeta, \quad -1/\gamma \le \zeta \le 1/\gamma \\
\Sigma_2(\zeta) &= \Sigma_1(\zeta) - 2 - 2E_1(\gamma\zeta - 1)/E, \quad 1/\gamma \le \zeta \le 1/2.
\end{aligned} \tag{11}$$

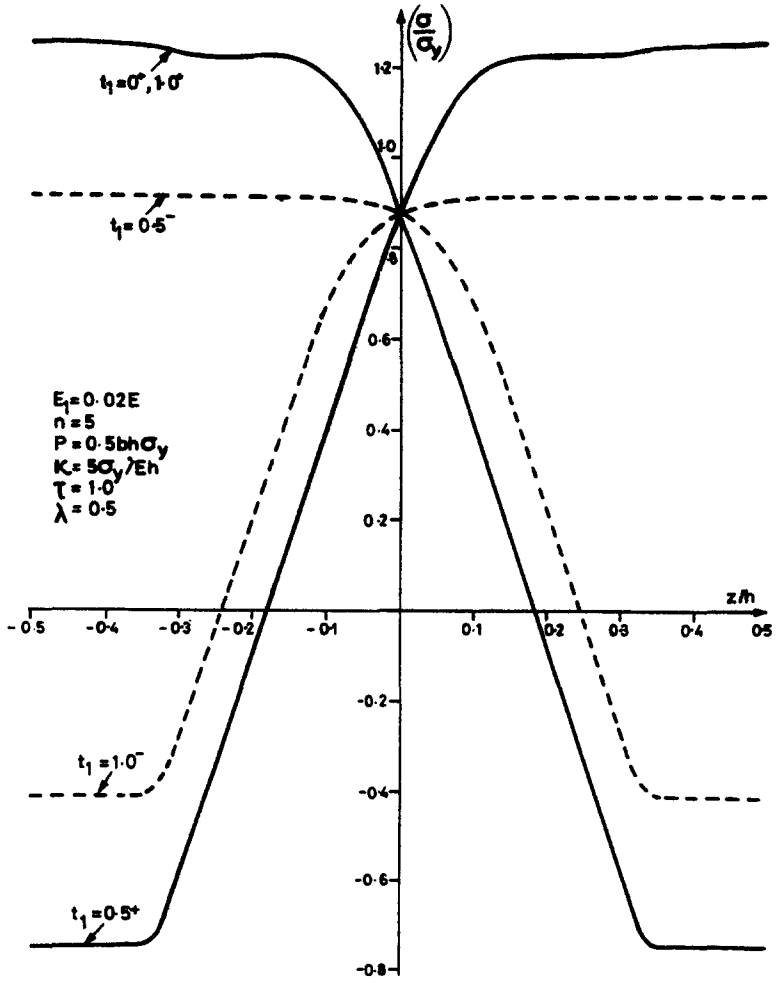

Fig. 3. Beam, cyclic stationary stress distributions.

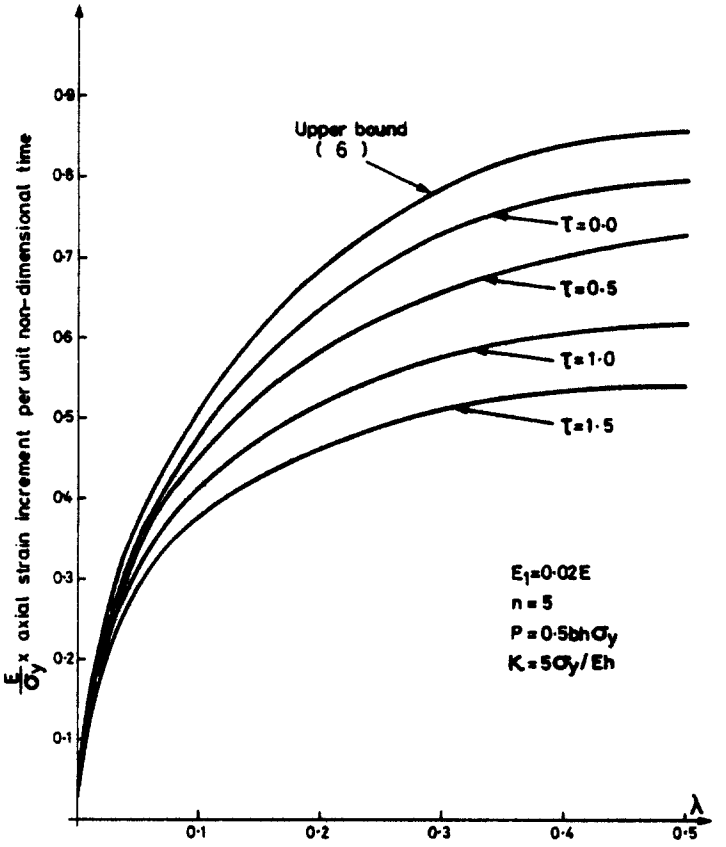

Fig. 4. Beam, comparison of exact, limiting and upper bound solutions.

For the case of perfect-plasticity ($E_1 = 0$) the constraints $|\Sigma_1| \le 1$ and $|\Sigma_2| \le 1$ must be applied. These require $\Sigma_2 = 1$, $\Sigma_1 = -1$ for $-1/2 \le \zeta \le -1/\gamma$ and $\Sigma_1 = 1$, $\Sigma_2 = -1$ for $1/\gamma \le \zeta \le 1/2$. In the absence of ratchetting, the displacement bound (6) is given in terms of Σ_1, Σ_2 as

$$\Delta(E\epsilon/\sigma_y) < \frac{1}{n}\left(\frac{n}{n+1}\right)^{n+1}\left(\frac{1}{\Sigma_R - \Sigma_P}\right)\int_{-1/2}^{1/2}[\lambda\Sigma_1^{n+1} + (1-\lambda)\Sigma_2^{n+1}]\,d\zeta$$

where $\Sigma_R = \int_{-1/2}^{1/2}\Sigma_1\,d\zeta$, $\Sigma_P = P/bh\sigma_y$ and $\Delta\epsilon$ is the increase in axial strain per unit non-dimensional time. Using the results of Section 5 of [4] the displacement bound was optimized as follows: Any initial estimate (for which, in the case of perfect plasticity, Σ_1 and Σ_2 satisfied the yield criterion) led from eqn (11) to a value of the upper bound proportional to W, say, where

$$W = \frac{1}{(\Sigma_R - \Sigma_P)}\int_{-1/2}^{1/2}[\lambda\Sigma_1^{n+1} + (1-\lambda)\Sigma_2^{n+1}]\,d\zeta$$

Following eqn (30) of [4], for this value of W a new stress distribution $\Sigma_1(\zeta)$ was chosen so that its corresponding creep displacement satisfied

$$\lambda\Sigma_1^n + (1-\lambda)\Sigma_2^n = W/(n+1)$$

for all ζ. For perfect plasticity, the resultant values of Σ_1, Σ_2 were amended if they violated the yield criterion. For instance, if the new value $\Sigma_1 > 1$ then Σ_1 was set at $\Sigma_1 = 1$; if $\Sigma_2 < -1$ then $\Sigma_2 = -1$; etc. Having determined new values of Σ_1, Σ_2, a new value of W was evaluated and hence new values of Σ_1, Σ_2 obtained as above. This process converged rapidly to the optimum bound, four iterations being adequate. The limiting solution for cycle time $\tau \to 0$ was obtained in a similar iterative manner.

Optimum upper bound solutions and limiting ($\tau \to 0$) solutions are compared with exact

solutions in Fig. 4. For the results plotted, the yield zones of the cyclic plasticity solutions occupy a fifth of the total depth h of the beam. The upper bound and limiting solution were obtained fairly readily whereas the evaluation of exact solutions required large amounts of computing time before a cyclic stationary state was reached.

For realistic structures, the creep strain accumulated in the cyclic stationary state is limited to about 1%, i.e. to about ten yield strains. Assuming that the structure must withstand more than 200 cycles in its lifetime, the non-dimensional cycle time ($E\dot{V}_0\tau/\sigma_y$) must be less than 0.5 for small values of λ and less than 0.01 for values of λ nearer 0.5 (see Fig. 4). It can be seen that, for such cycle times both the upper bound and limiting ($\tau \to 0$) solutions give good estimates of the true behaviour.

The optimum bound (6) and the limiting solution ($\tau \to 0$) have also been evaluated for a beam of perfectly-plastic material ($E_1 = 0$ in Fig. 1). Consideration is limited to cases where ratchetting does not occur. This requires that the applied load P and the curvature change κ satisfy $P\kappa < 2b\sigma_y^2/E$, (Bree [6]). In addition the upper bound solutions are ones for which there is no ratchetting so that additional loads R satisfy $(P+R)\kappa < 2b\sigma_y^2/E$.

Some typical results are given in Table 1. The difference between the two solutions is much greater than in the hardening case and, for low values of axial load P, the upper bound gets a lot worse. This is because the stress in the outer one-fifth of the beam must be $\pm\sigma_y$ for the plasticity solution. These regions contribute a large fraction of the integral (6) and so the upper bound is much less sensitive to axial load variations than the actual solution.

3.2 *Thin-walled tube*

Consider the thin-walled tube shown in Fig. 5 subjected to a constant axial load (giving rise to a constant mean axial stress σ_s) and to a constant internal pressure p (giving rise to a constant mean hoop stress σ_p). A temperature difference is imposed between the inner and outer surfaces of the tube and has the periodic variation shown in Fig. 5. It is assumed that the temperature difference gives rise to a temperature distribution which is linear in the radial co-ordinate, z. The deformation is completely described by two displacement components, an axial displacement independent of radius and a radial displacement which gives rise to a hoop strain approximately independent of radius (since thickness $h \ll$ radius R). The effect of temperature on creep rate is not considered and so the problem is similar in nature to that of the beam. The structure is used to demonstrate the use of the hardening law and the upper bound method for two-dimensional stress systems.

Exact solution. The function ϕ in the creep law (2) is taken as the von Mises equivalent stress. The elastic and creep strain rates are then given from eqn (2) and Hooke's law by

$$E\dot{e}_x = \dot{\sigma}_x - \nu\dot{\sigma}_\theta, \quad E\dot{e}_\theta = \dot{\sigma}_\theta - \nu\dot{\sigma}_x$$
$$\dot{V}_x = \dot{V}_0(\sigma_e/\sigma_y)^{n-1}(\sigma_x - \tfrac{1}{2}\sigma_\theta)/\sigma_y, \quad \dot{V}_\theta = \dot{V}_0(\sigma_e/\sigma_y)^{n-1}(\sigma_\theta - \tfrac{1}{2}\sigma_x)/\sigma_y \tag{12}$$

where suffices x, θ denote axial and hoop components respectively, ν is Poisson's Ratio and σ_e is the equivalent stress, $\sigma_e^2 = \sigma_x^2 + \sigma_\theta^2 - \sigma_x\sigma_\theta$. The numerical results have been obtained for a value of Poisson's Ratio $\nu = 0.3$. The conditions of constant mean axial stress, constant mean hoop stress and of total axial and hoop strains being independent of radius readily lead to the

Table 1. Perfectly-plastic beam, comparison of non-dimensional strain rates

	λ					
	0.0	0.1	0.2	0.3	0.4	0.5
$\Sigma_p = 0.1$, $\gamma = 2.5$						
Limiting solution ($\tau \to 0$)	0.001	0.008	0.011	0.013	0.013	0.014
Optimum bound (6)	0.110	0.119	0.127	0.133	0.137	0.139
$\Sigma_p = 0.25$, $\gamma = 2.5$						
Limiting solution ($\tau \to 0$)	0.095	0.094	0.120	0.134	0.142	0.144
Optimum bound (6)	0.283	0.289	0.292	0.293	0.293	0.293

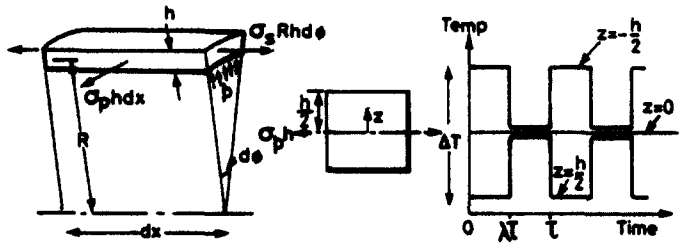

Fig. 5. Geometry and loading of thin tube.

required results for periods of creep at constant temperature,

$$\dot{\epsilon}_x = \int_{-1/2}^{1/2} \dot{V}_x \, d\zeta \quad \dot{\epsilon}_\theta = \int_{-1/2}^{1/2} \dot{V}_\theta \, d\zeta$$

$$\dot{\sigma}_x = \frac{E}{(1-\nu^2)} \int_{-1/2}^{1/2} (\dot{V}_x + \nu \dot{V}_\theta) \, d\zeta - \frac{E}{(1-\nu^2)} (\dot{V}_x + \nu \dot{V}_\theta) \tag{13}$$

$$\dot{\sigma}_\theta = \frac{E}{(1-\nu^2)} \int_{-1/2}^{1/2} (\dot{V}_\theta + \nu \dot{V}_x) \, d\zeta - \frac{E}{(1-\nu^2)} (\dot{V}_\theta + \nu \dot{V}_x)$$

where the non-dimensional co-ordinate $\zeta = z/h$ has been introduced. It has been assumed that no further plastic strains occur during periods of creep at constant temperature (an assumption valid for the conditions considered). Equations (12) and (13) have been solved using the method of time-steps in conjunction with the fourth-order Runge–Kutta method given by eqn (10).

The above elastic-creep analysis must be interrupted at times of temperature change by an elastic-plastic analysis. The yield criterion (4) may be written in terms of the constants σ_y, E_1 of Fig. 1 as

$$\bar{\sigma}_x^2 + \bar{\sigma}_\theta^2 - \bar{\sigma}_x \bar{\sigma}_\theta \leq \sigma_y^2$$

where

$$\bar{\sigma}_x = \sigma_x - 4E_1(p_x + \tfrac{1}{2}p_\theta)/3 \tag{14}$$
$$\bar{\sigma}_\theta = \sigma_\theta - 4E_1(p_\theta + \tfrac{1}{2}p_x)/3$$

which is a translation of the Mises ellipse in the σ_x, σ_θ plane. The flow rule (4) is

$$\dot{p}_x/\dot{p}_\theta = (\bar{\sigma}_x - \tfrac{1}{2}\bar{\sigma}_\theta)/(\bar{\sigma}_\theta - \tfrac{1}{2}\bar{\sigma}_x). \tag{15}$$

In order to solve the elastic-plastic problem, the temperature change ΔT must be divided into a number of intervals δT (ten intervals were found to be adequate). The change in total strain is then given from eqn (1) as

$$\delta\epsilon_x = \delta e_x + \delta p_x - \alpha\zeta\delta T; \quad \delta\epsilon_\theta = \delta e_\theta + \delta p_\theta - \alpha\zeta\delta T \tag{16}$$

where $\delta\epsilon_x$, $\delta\epsilon_\theta$ are independent of ζ. For any given estimates of $\delta\epsilon_x$, $\delta\epsilon_\theta$ the changes in $\delta\sigma_x$, $\delta\sigma_\theta$ which would occur elastically ($\delta p_x = \delta p_\theta = 0$) can be evaluated using eqn (16). Where the elastic changes do not cause the yield criterion (14) to be violated, the changes in stress have their elastic values and $\delta p_x = \delta p_\theta = 0$. Where the elastic changes cause (14) to be violated, use of the flow rule (15) and the condition that the final state must lie on the yield surface enable δp_x, δp_θ to be related to $\delta\sigma_x$, $\delta\sigma_\theta$. The changes $\delta\sigma_x$, $\delta\sigma_\theta$ can then be obtained from eqn (16). An iterative method was used to find those values of $\delta\epsilon_x$, $\delta\epsilon_\theta$ for which the mean stress changes were zero. Details of the numerical procedure are omitted for brevity.

Combination of the above elastic-creep and elastic-plastic analyses enables the cyclic stationary state to be obtained by convergence from any initial stress distribution. For

comparison purposes, the cyclic stationary state is characterised by the non-dimensional work or generalised displacement rate U given by

$$U = \left(\frac{\sigma_p}{\sigma_y}\right)\left(\frac{E\Delta\epsilon_\theta}{\sigma_y}\right) + \left(\frac{\sigma_s}{\sigma_y}\right)\left(\frac{E\Delta\epsilon_x}{\sigma_y}\right) \tag{17}$$

where $\Delta\epsilon_x$, $\Delta\epsilon_\theta$ are mean axial and hoop strain increments per unit non-dimensional time. Some results are presented in Fig. 6 for a range of non-dimensional cycle time τ and for a range of the cycle parameter λ.

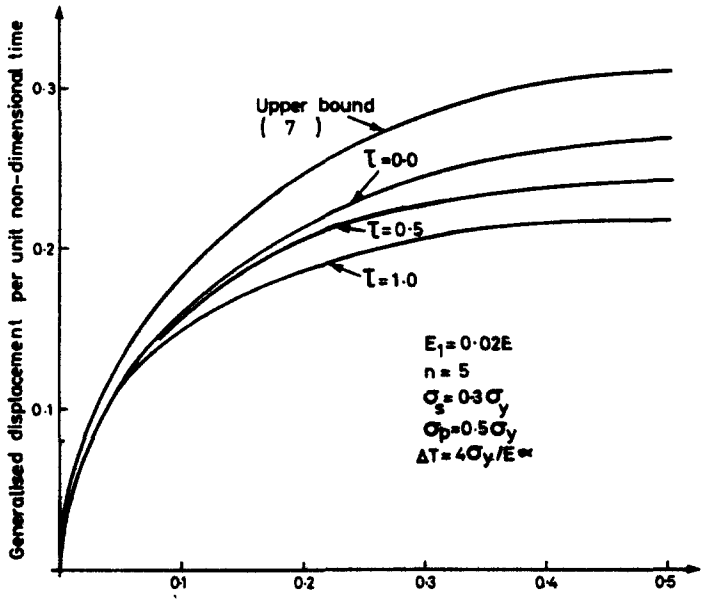

Fig. 6. Tube, comparison of exact, limiting and upper bound solutions.

Upper work bound. In order to determine the work bound (7) it is necessary to find the form of the cyclic plasticity solution. This consists of an elastic core where no yielding occurs and yield zones where equal and opposite amounts of plastic strain occur on application and removal of the temperature difference. For the temperature change, it can be seen from eqns (12) and (16) that for purely elastic behaviour ($\delta p_x = \delta p_\theta = \delta\epsilon_x = \delta\epsilon_\theta = 0$) $\delta\sigma_x = \delta\sigma_\theta$, i.e. that the elastic loading line is parallel to the major axis of the Mises ellipse. As a result of plastic deformation the Mises ellipse is translated but not rotated in the σ_x, σ_θ plane and consequently in the yield zones for the cyclic plasticity solution, loading occurs along the major axis of the Mises ellipse. This is shown schematically in Fig. 7. Starting from the point A^1 on the dashed ellipse, elastic changes occur until the point B^1 is reached. Plasticity then occurs from B^1 to B and the yield surface moves from the dashed ellipse to the solid ellipse. On reversal of the temperature difference, changes are elastic from B to A and plasticity occurs from A to A^1 returning the yield surface to its original position.

When yielding occurs, the changes in plastic strain are then simply related to the stress changes from eqns (14) and (15) by

$$\delta\sigma_x = \delta\sigma_\theta = 2E_1\delta p_x = 2E_1\delta p_\theta \tag{18}$$

The overall changes in σ_x, σ_θ are then easily obtained in terms of the overall change in temperature difference ΔT from eqns (16) and (18). Introducing the non-dimensional temperature change $\gamma = E\alpha\Delta T/2\sigma_y(1-\nu)$, the elastic core is the region $|\zeta| \le 1/\gamma$. Denoting the non-dimensional stress distribution for the cyclic plasticity solution as $\Sigma_1(\zeta)$ for $0 < t_1 < \lambda\tau$ and

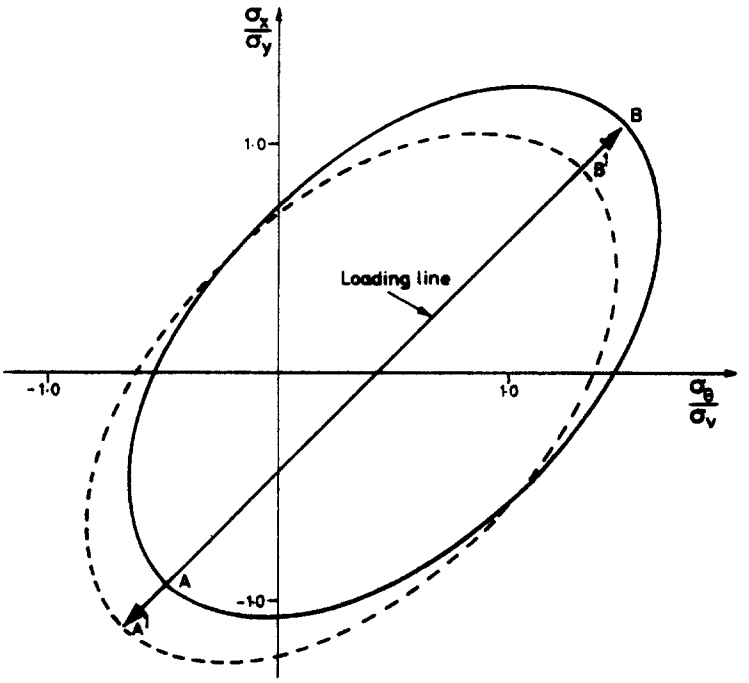

Fig. 7. Loading surfaces for cyclic plasticity solution.

as $\Sigma_2(\zeta)$ for $\lambda\tau < t_1 < \tau$ then

$$\left.\begin{aligned}
\Sigma_2 &= \Sigma_1 - 2 + 2(1+\gamma\zeta)\left[\frac{2E_1(1-\nu)}{E+2E_1(1-\nu)}\right], && -\tfrac{1}{2} \le \zeta \le -1/\gamma \\
\Sigma_2 &= \Sigma_1 + 2\gamma\zeta, && -1/\gamma \le \zeta \le 1/\gamma \\
\Sigma_2 &= \Sigma_1 + 2 - 2(1-\gamma\zeta)\left[\frac{2E_1(1-\nu)}{E+2E_1(1-\nu)}\right], && 1/\gamma \le \zeta \le \tfrac{1}{2}
\end{aligned}\right\} \tag{19}$$

Here Σ_1, Σ_2 can represent either σ_x/σ_y or σ_θ/σ_y but different choices of $\Sigma_1(\zeta)$ are required to satisfy equilibrium requirements. Denoting the corresponding values of Σ_1 as Σ_{1x}, $\Sigma_{1\theta}$ with equivalent stress Σ_{1e}, the work bound (7) may be written in terms of the generalized displacement U of eqn (17) as

$$\left.\begin{aligned}
U &\le \frac{1}{(\mu-1)n}\left(\frac{n}{n+1}\right)^{n+1} \int_{-1/2}^{1/2} \{\lambda \Sigma_{1e}^{n+1} + (1-\lambda)\,{}^{n+1}_{2e}\}\,\mathrm{d}\zeta \\
\text{where} \quad \mu &= \int_{-1/2}^{1/2} \Sigma_{1\theta}\,\mathrm{d}\zeta/\sigma_p = \int_{-1/2}^{1/2} \Sigma_{1x}\,\mathrm{d}\zeta/\sigma_z
\end{aligned}\right\} \tag{20}$$

The associated strain cycles (8), β_x, β_θ say, are

$$\left.\begin{aligned}
\beta_x &= \lambda\Sigma_{1e}^{n-1}(\Sigma_{1x} - \tfrac{1}{2}\Sigma_{1\theta}) + (1-\lambda)\Sigma_{2e}^{n-1}(\Sigma_{2x} - \tfrac{1}{2}\Sigma_{2\theta}) \\
\beta_\theta &= \lambda\Sigma_{1e}^{n-1}(\Sigma_{1\theta} - \tfrac{1}{2}\Sigma_{1x}) + (1-\lambda)\Sigma_{2e}^{n-1}(\Sigma_{2\theta} - \tfrac{1}{2}\Sigma_{2x})
\end{aligned}\right\} \tag{21}$$

where the condition at the optimum is that β_x and β_θ are independent of ζ.

Since the applied loads are constant, the other condition at the optimum is similar to eqn (30) of [4] and is related to the bound (20) by W, say,

$$W = (n+1)\left[\beta_x\left(\frac{\sigma_z}{\sigma_y}\right) + \beta_\theta\left(\frac{\sigma_p}{\sigma_y}\right)\right] \tag{22}$$

where

$$W = \frac{1}{(\mu - 1)} \int_{-1/2}^{1/2} \{\lambda \Sigma_{1e}^{n+1} + (1 - \lambda)\Sigma_{2e}^{n+1}\} \, d\zeta. \tag{23}$$

The following iterative procedure to obtain the optimum bound was adopted.

Initial estimates Σ_{1_x}, $\Sigma_{1\theta}$ which satisfied eqn (20) enabled W to be evaluated from eqns (19) and (23). For this value of W, new values of Σ_{1_x}, $\Sigma_{1\theta}$ were chosen so that eqn (20) was satisfied and so that β_x, β_θ given by (21) were independent of ζ and satisfied (22). The new values of Σ_{1_x}, $\Sigma_{1\theta}$ led to a new value of W from eqns (19) and (23) and hence to further estimates of Σ_{1_x}, $\Sigma_{1\theta}$. The process was repeated to convergence. The limiting solution for cycle time $\tau \to 0$ was found in a similar iterative manner.

The optimum works bounds (7) and the limiting solutions ($\tau \to 0$) are compared with exact solutions in Fig. 6. As in the case of the beam, the bounds and limiting solutions were evaluated fairly readily whilst the exact solutions required large amounts of computing time before a cyclic stationary state was reached.

The limitation on accumulated creep strain in practical structures suggests that a typical non-dimensional cycle time is about $\tau = 0.25$. It can be seen From Fig. 6 that, for such cycle times, both the upper bound method and the limiting solution ($\tau \to 0$) give good estimates of the true behaviour.

3.3 *Two-bar structure*

Consider the structure shown in Fig. 8 consisting of two bars of equal cross-sectional area A and of equal length, l. A constant vertical load P is applied and the structure is constrained to move vertically. The temperature of bar 2 is held constant while the temperature of bar 1 varies periodically as shown in Fig. 8. The bars are made of perfectly-plastic material and the structure is used to assess the accuracy of the upper bound method in cases of ratchetting.

The non-dimensional parameters $\Sigma_p = P/2A\sigma_y$ and $\Sigma_T = E\alpha\Delta T/\sigma_y$, where α is the coefficient of thermal expansion, are used to describe the loading. The temperature effect on creep rate $g(\theta)$ of eqn (2) is represented by the constant F which is the factor by which the creep rate increases for a temperature increase ΔT.

Exact solution ($\tau \to 0$). The exact solution for cycle time $\tau \to 0$ can be determined immediately. After bar 1 heats up ($t = 0^+$) the stress in bar 2 must be equal to the yield stress σ_y, i.e. $\Sigma_2(0^+) = 1$. From conditions of compatibility and equilibrium, the displacement and stress rates, $\dot{u}$, $\dot{\Sigma}_2$, at this time are

$$\begin{aligned} \beta(0^+) &= E\dot{u}(0^+)/l\sigma_y = (E\dot{V}_0/2\sigma_y)\{1 + F(2\Sigma_p - 1)^n\} \\ \dot{\Sigma}_{2(0^+)} &= -(E\dot{V}_0/2\sigma_y)\{1 - F(2\Sigma_p - 1)^n\} \end{aligned} \tag{24}$$

where $\dot{\beta}$ is the non-dimensional displacement rate and eqns (24) are only valid if they give $\dot{\Sigma}_2 < 0$. Attention is restricted to cases where $\dot{\Sigma}_2(0^+)$ is negative as given above, which is true for any value of F if $\Sigma_p \leq 0.5$. Assuming that stress redistribution is small in the time $0 < t < \lambda\tau$, the strain incurred in this part of the cycle is $\lambda\tau\dot{\beta}(0^+)$ and the stress in bar 2 immediately before the temperature change at time $\lambda\tau$ is $\Sigma_2(\lambda\tau^-) = 1 + \lambda\tau\dot{\Sigma}_2(0+)$. Immediately after the temperature

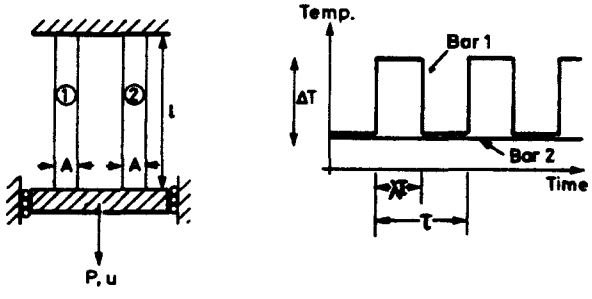

Fig. 8. Geometry and loading of two-bar structure.

change, the stress in bar 1 is the yield stress and hence the stress in bar 2 is $\Sigma_2(\lambda\tau^+) = 2\Sigma_p - 1$. Since no plastic strain occurs in bar 2 at this time, the strain change due to the temperature change is

$$\beta(\lambda\tau^+) - \beta(\lambda\tau^-) = \Sigma_2(\lambda\tau^+) - \Sigma_2(\lambda\tau^-) = 2\Sigma_p - 1 - 1 - \lambda\tau\dot{\Sigma}_2(0^+)$$

The strain change due to creep between time 0^+ and $\lambda\tau^-$ is $\lambda\tau\dot{\beta}(0^+)$ and hence from eqns (24)

$$\beta(\lambda\tau^+) - \beta(0^+) = 2\Sigma_p - 2 + E\lambda\tau\dot{V}_0/\sigma_y.$$

In similar manner the change between times $\lambda\tau^+$, τ^+ is

$$\beta(\tau^+) - \beta(\lambda\tau^+) = \Sigma_T + 2\Sigma_p - 2 + E(1-\lambda)\tau\dot{V}_0/\sigma_y.$$

The total change per cycle $\beta(\tau^+) - \beta(0^+) = \Delta\beta$, say, is then

$$\Delta\beta = \Sigma_T + 4\Sigma_p - 4 + E\tau\dot{V}_0/\sigma_y = \Delta U_p + \Delta U_c,$$

say, where ΔU_p is the ratchet displacement per cycle in the absence of creep. It should be noted that, in the presence of creep, the displacement increase due to plasticity is greater than ΔU_p. It can be seen that the increase per cycle is independent of the parameters λ, F.

Upper bound. The cyclic plasticity solution for this problem is shown in Fig. 9. The stress in bar 2 is σ_y for $0 < t < \lambda\tau$ and in bar 1 is σ_y for $\lambda\tau < t < \tau$. The stress distribution is then completely defined from equilibrium considerations and the upper displacement bound (6) can only be optimised for an additional load R ($=(\mu-1)P$ say). The upper bound (6) is then

$$\Delta\beta \le 4\mu\Sigma_p - 4 + \Sigma_T + \frac{1}{n}\left(\frac{n}{n+1}\right)^n \frac{\Delta U_c}{(2(\mu-1)\Sigma_p)}[1 + \{2\mu\Sigma_p - 1\}^{n+1}(\lambda F + 1 - \lambda)]$$

where $\Delta U_c = E\tau\dot{V}_0/\sigma_y$ as defined above. Although the bound involves the parameters λ, F, the optimum solution occurs at values of μ for which $(2\mu\Sigma_p - 1)^{n+1} \ll 1$ and is virtually independent of λ, F. This is in agreement with the exact solution $\tau \to 0$ given above.

The upper bound and the exact solution ($\tau \to 0$) are compared in Table 2 for a variety of ΔU_p, ΔU_c, i.e. for a variety of cycle times. In view of the severe loading, agreement between the two solutions is good.

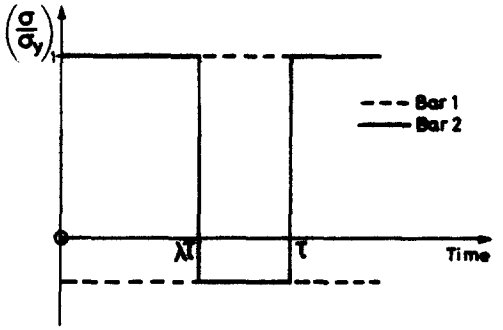

Fig. 9. Two-bar, cyclic plasticity solution.

Table 2. Two-bar, comparison of non-dimensional strain increments

ΔU_p	0.02	0.05	0.10	0.02	0.05	0.10
ΔU_c	0.05	0.05	0.05	0.10	0.10	0.10
Exact ($\tau \to 0$)	0.07	0.10	0.15	0.12	0.15	0.20
Bound (6)	0.18	0.21	0.26	0.25	0.28	0.33

4. DISCUSSION

Upper bounds on displacement, work and creep energy dissipation have been applied to three structures. The bounds give a good estimate of the true behaviour for realistic cycle times. However, the accuracy of the displacement and work bounds becomes poor when there are large variations in imposed strains combined with low mechanical loads. This limitation of the upper displacement and work bounds will also apply for loading below the shakedown limit.

The upper bound on creep energy dissipation does not suffer from this restriction. As for loading below the shakedown limit, the optimum stress history should closely approximate the actual stress history for practical structures. Although the upper bound solution cannot guarantee to give a safe estimate of any particular displacement, it is, on average, safe.

For the cases considered, exact solutions required large amounts of computing time before a cyclic stationary state was reached whereas the optimum upper bounds could be readily evaluated. This was because the form of the cyclic plasticity solution could be easily obtained. However, for complex structures, the evaluation of a cyclic plasticity solution may prove to be difficult. Many perfectly-plastic structures settle down to a cyclic stress state after one cycle, but for cases of kinematic hardening the cyclic stress state is often approached only asymptotically. However, one cyclic plasticity solution may be used to provide upper bounds for a range of problems. Hence, when the behaviour of a complex structure is required for a variety of loading conditions, it should be worthwhile to evaluate the cyclic plasticity solution and use the upper bound approach.

Acknowledgements—I thank Professor W. S. Hemp, Department of Engineering Science, University of Oxford, for his assistance and encouragement in this work. This paper is published by permission of the Central Electricity Generating Board.

REFERENCES

1. F. K. G. Odqvist, *Mathematical Theory of Creep and Creep Rupture*. Second Edn, Oxford University Press, Oxford (1974).
2. F. A. Leckie, A review of bounding techniques in shakedown and ratcheting at elevated temperature. *Welding Research Council Bulletin* 195, 1 (1974).
3. A. R. S. Ponter, Deformation, displacement and work bounds for structures in a state of creep and subject to variable loading, *J. Appl. Mech.* **39**, 953 (1972).
4. R. A. Ainsworth, Bounding solutions for creeping structures subjected to load variations above the shakedown limit. *Int. J. Solids Structures* 13, 971–980 (1977).
5. R. K. Penny and D. L. Marriott, *Design for Creep*. McGraw-Hill, New York (1971).
6. J. Bree, Elastic-plastic behaviour of thin tubes subjected to internal pressure and intermittent high-heat fluxes with application to fast-nuclear-reactor fuel elements. *J. Strain Analysis* 2, 226 (1967).